IET Power Electronics

Research Article

IET Journals
The Institution of Engineering and Technology

Electromagnetic interference frequencies prediction model of flyback converter for snubber design

ISSN 1755-4535
Received on 4th July 2014
Accepted on 6th January 2015
doi: 10.1049/iet-pel.2014.0250
www.ietdl.org

Marcin Rucinski, Piotr Musznicki ✉, *Piotr J. Chrzan*

Faculty of Electrical and Control Engineering, Gdansk University of Technology, G.Narutowicza 11/12 80-233 Gdansk, Poland
✉ *E-mail: piotr.musznicki@pg.gda.pl*

Abstract: Snubber design for flyback converters usually requires experimental prototype measurements or simulation based on accurate and complex models. In this study simplified circuit modelling of a flyback converter has been described to dimension snubbers in early stage of design process. Simulation based prediction of the transistor and diode ringing frequencies has been validated by measurements in a prototype setup. In that way obtained simulation data enabled fast and precise snubbers dimensioning. Application example has illustrated effectiveness of the proposed methodology by line impedance stabilisation network (LISN) spectra evaluation of the experimental flyback converter resulting from snubbers dimensioning.

1 Introduction

Flyback converters are commonly used in industrial switch mode power supply because of their simplicity, high efficiency, low cost and transformer isolation between input and output. However in modern converters, the trend for increasing switching frequency is connected with increasing electromagnetic interference (EMI) caused by high-voltage spikes with ringing oscillations at transistor and diode turn-off transients. One of the most effective method of EMI reducing is application of snubbers. It can be noted that designing procedure requires precise evaluation of the ringing frequency generated during semiconductor switches commutation and the value of the transformer leakage inductance. The most popular and practical way is to measure these oscillations during laboratory tests – but it requires working prototype – or it can be forecast from models. EMI disturbances prediction for snubber application can be obtained by precise modelling and simulation of a flyback converter [1–6]. However, this time consuming methodology requires extraction of parasitic parameters of main circuit component including semiconductor switches, high-frequency power transformer and PCB layout. Moreover, dependence of these parasitic parameters on electric and magnetic field couplings is difficult to identify at the design stage of a converter [7]. In another similar approach aiming to develop wide band flyback converter model [8], library switch models of the OrCAD circuit simulator were used and power transformer parasitic parameters were derived from the LCR meter direct measurements. However instead of snubber circuits, the spread spectrum technique was recommended. For a converter electromagnetic compatibility (EMC) analysis, if calculation speed is preferred over high precision, a technique based on the state vector approach and a simple switch device model has been proposed in [9, 10]. Experimental flyback converter study in [11] signalled a turn-off ringing phenomena mainly caused by the resonant oscillating of transformer leakage inductance with the MOSFET's output capacitance. To verify above observation in a quantitative manner, in this paper fast and accurate method of ringing frequency identification has been considered.

The flyback converter model using simplified equivalent circuit is developed (Section 2) and validated (Section 3). However, it should be noted that presented modelling method is not sufficient to forecast the EMI noise levels. Results of simulation carried out in the circuit simulator *Synopsys Saber@Sketch* are compared with experimentation in a laboratory setup. Transistor voltage V_{ds} and diode voltage V_d frequency spectra, evaluated using fast Fourier transform (FFT) are utilised to indicate accurate ringing frequencies for converter without snubbers. Next – in Section 4 – snubbers application example is presented.

2 EMI frequencies prediction model

In a fundamental flyback converter (Fig. 1*a*), EMI disturbances are mainly generated at transistor and diode terminals close to connection points of transformer [12–15]. During energy transfer from the primary to secondary, each commutation excites voltage and current damped oscillation between switch capacitances and transformer leakage inductances. To construct simplified converter model for EMI ringing frequencies extraction (Fig. 1*b*), the following assumptions based on extensive simulation study have been taken into account:

- continuous current conduction mode (CCM) operation of the flyback converter is considered,
- transformer secondary side parameters denoted with the prime sign are referred to primary using the turns ratio $n = n_1/n_2$.
- the high-frequency transformer equivalent circuit [16] consists of magnetising inductance L_{1m}, total primary, and secondary leakage inductance L_{leak}, winding resistances R_1, R_2 (inserted separately for improving numerical stability, conditions of the simulation model), primary C_{w1} and secondary C_{w2} windings lumped capacitances,
- the capacitance C_{w1} takes a part in oscillation generation during transistor commutation (f_{rT}) whereas C'_{w2} contributes to diode commutation (f_{rD}),
- it has been investigated by simulation that transformer winding-to-winding capacitances have negligible influence on ringing frequency, however they contribute to common mode current propagation paths [17], hence they have not been inserted in frequencies prediction model (Fig. 1*b*),
- printed circuit board (PCB) layout parasitics are neglected because of dominant impact on disturbances frequencies of leakage inductances and semiconductor parasitic capacitances,
- input electrolytic capacitor C_{in}, output filter L_{out}–C_{out2} and load R_l are omited since they are negligible in ringing frequencies circuits,
- output filter capacitance $C_{out1} \gg C_j$ has a neglected impact on ringing frequencies,
- the MOSFET model comprises ideal switch with parasitic capacitances: $C_{gd} = C_{rss}$, $C_{gs} = C_{iss} - C_{rss}$, $C_{ds} = C_{oss} - C_{rss}$, where

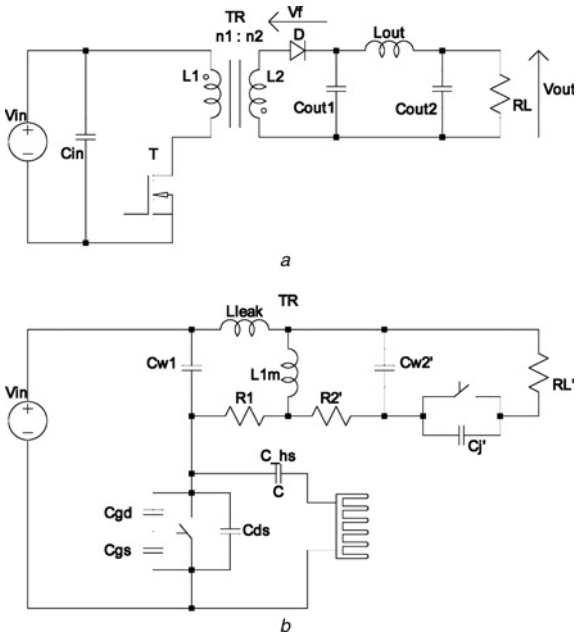

Fig. 1 *Flyback converter*

a Principal scheme
b EMI frequencies prediction model

C_{rss}, C_{iss}, C_{oss} are derived from the datasheet, as a function of drain – source voltage $V_{ds} = V_{in} + (V_{out} + V_f)n$ at the turn-off interval,

- parasitic capacitance C_{hs} between the MOSFET and heat sink, connected to the primary ground potential, contributes to the ringing frequency and is added to MOSFET capacitances (parallel connection),
- secondary diode model is applied based on the space charge layer capacitance C_j [18]; referring secondary circuit to the primary yields

$$C_j' = \frac{C_{j0}}{(1 + (V_R/\phi))^{1/2} n^2} \tag{1}$$

where, ϕ is diffusion potential (for silicon diode 0.6–0.8 V), V_R is reverse voltage (defined positive), C_{j0} is capacitance at zero applied voltage (parameter from datasheet),

- in the secondary circuit, capacitance between Schottky diode and heat sink is parallel connected with output filter capacitor, therefore it has no influence on ringing frequency.

The transformer parasitic capacitances have been estimated using digital adaptive Wiener filter (WF) [19]. First, current and voltage have been measured, by applying the square wave voltage generator to the transformer primary, secondary and between primary and secondary terminals. Based on the obtained data, the filter has been adapted to identify transformer impedance in the form of WF transfer function. This allowed the inner resonant

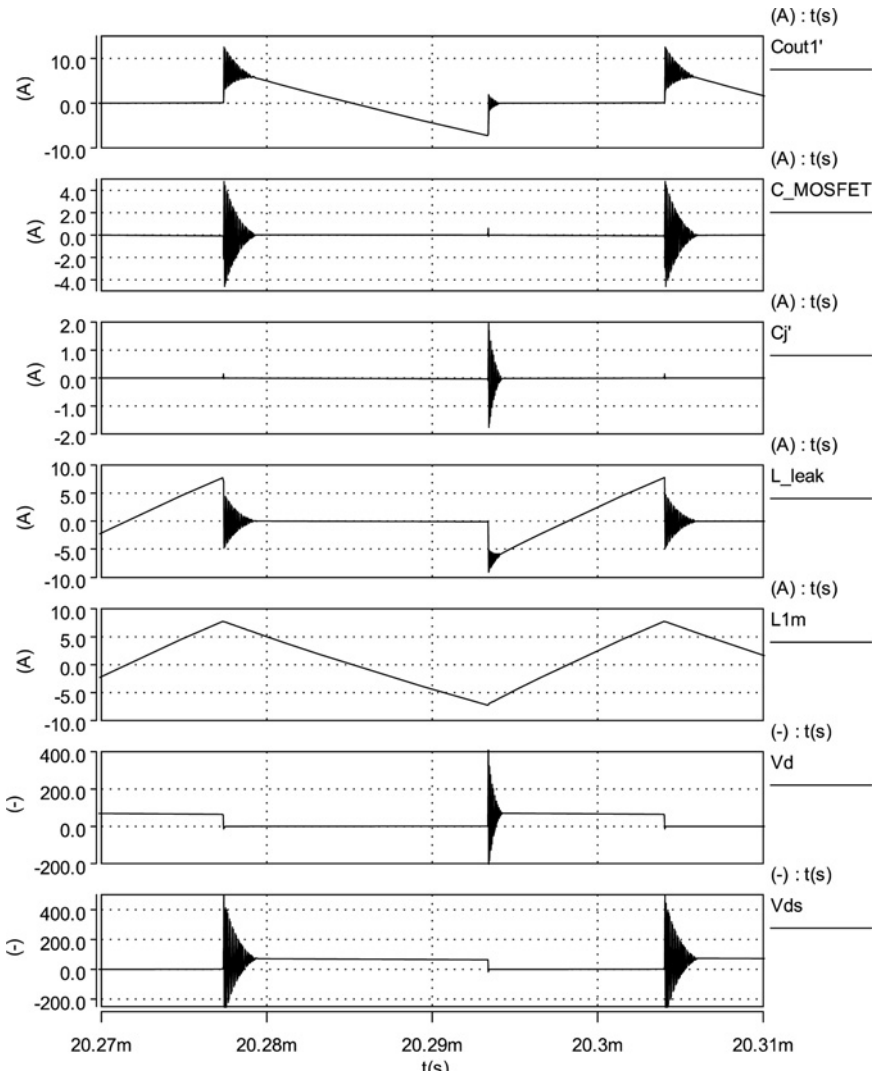

Fig. 2 *Simulation model (Fig. 1b) waveforms*

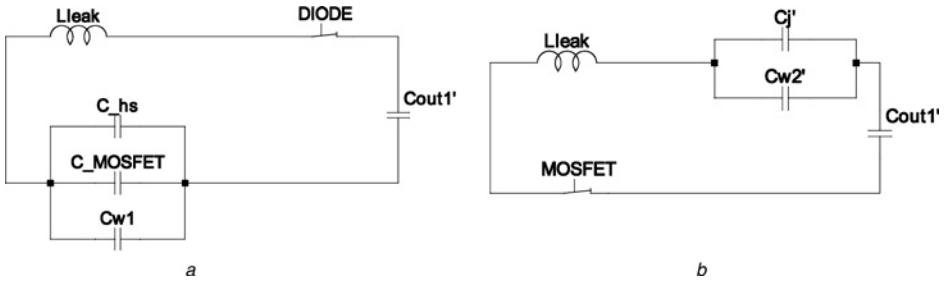

Fig. 3 *Simplified flyback converter resonance circuit modes*

a MOSFET turn-off and diode turn-on
b Diode turn-off and MOSFET turn-on

frequencies to be identified and this was used to approximate the $C_{w1} \simeq 10$ pF and $C_{w2} \simeq 1$ pF.

In Fig. 2, simulation waveforms of the simplified converter model (Fig. 1*b*) indicate ringing circuit paths during the diode and the MOSFET turn-off. Dominant impact on ringing circuits parameters and frequencies have the transformer leakage inductance L_{leak} with, respectively, diode capacitance C_j and MOSFET equivalent capacitance C_{MOSFET}. It can be notice that magnetising inductance (obviously in CCM) have no influence on ringing frequencies and EMI propagation.

Finally, analytical model for a resonance turn-off frequency evaluation can be simplified to the two converter states (Fig. 3). Ringing frequency in both states result from equivalent values of parasitic inductance L_{leak} and total of semiconductor capacitances. Thus, the MOSFET turn-off yields

$$f_{\text{rT}} = \frac{1}{2\pi\sqrt{L_{\text{leak}}(C_{\text{hs}} + C_{\text{MOSFET}} + C_{w1})}} \tag{2}$$

where $C_{\text{MOSFET}} = C_{\text{ds}} + C_{\text{gs}} \| C_{\text{gd}}$ and since $C'_{\text{out1}} \gg (C_{\text{hs}} + C_{\text{MOSFET}} + C_{w1})$, it has been neglected. Respectively, for the diode turn-off ringing frequency one obtains

$$f_{\text{Dr}} = \frac{1}{2\pi\sqrt{L_{\text{leak}}(C'_j + C'_{w2})}} \tag{3}$$

3 Model validation

Prototype flyback converter was built adequately to the parameter specification as in Table 1. It corresponds to a typical sizing of 48 Volt DC/DC converters used in telecommunications network equipment [20]. To realise converter switching operation, the FDB2572 N-channel Power Trench MOSFET and the NTST20120CTG trench based Schottky rectifier were chosen. The semiconductor switches parasitic capacitances resulting from converter operation conditions are indicated in Table 2. The pulse transformer winding was performed using sandwiched winding technique with flat *Litz* wire to decrease the leakage inductance [21]. The converter was controlled using UC3842 current mode PWM driver at the fixed frequency $f_s = 37$ kHz in the CCM with transistor current sense in closed control loop. In Fig. 4 is shown a general view of the EMI noise measurement setup consisting of the flyback converter with load resistors and the two-line V-network line impedance stabilisation network (LISN) device. Converter parameters for simulation model were obtained from the experimental prototype setup. Simulation research was carried out using *Synopsys Saber* circuit simulator. However, it should be noticed, that for a required analysis any other circuit simulator, for example, Spice also could be applied.

Both, simulation model and prototype converter were tested at the same operating conditions (Table 1) at $i_{\text{out}} = 7$ A. Measurements of transistor and diode voltages have been recorded with the aid of Tektronix DPO 4034 digital oscilloscope. The MOSFET drain-source voltage V_{ds} waveforms and the secondary diode voltage V_d waveforms were transformed into the frequency domain by using the graphical waveform analyser *Synopsys Cosmo Scope*, as is depicted in Figs. 5 and 6.

Comparison of experimental spectra envelopes with those obtained by simplified model simulation confirms accurate

Table 1 Prototype converter parameters

Parameter	Value
input voltage	$V_{\text{in}} = 40 \div 50$, V
switching frequency	$f_s = 37$, kHz
rated output voltage	$V_{\text{out}} = 10$, V
rated output current	$i_{\text{out}} = 10$, A
primary inductance	$L1 = 29.2$, μH
secondary inductance	$L2 = 7.7$, μH
size and type of transformer core	EE42/21/15-3C90
turns ratio	$n = 2$
leakage inductances	$L1_l \simeq 0.36$, μH
	$L2_l \simeq 0.09$, μH
transformer lumped capacitance	$C_{w1} \simeq 10$, pF
	$C_{w2} \simeq 1$, pF

Table 2 Semiconductors parasitic capacitance values

Semiconductor	Value, pF
FDB2572 MOSFET ($V_{\text{ds}} = 62$ V)	$C_{\text{gd}} = 23$
	$C_{\text{ds}} = 86$
	$C_{\text{gs}} = 1680$
Transistor – heatsink capacitance	$C_{\text{hs}} = 4$
NTST20120CTG Schottky diode ($\phi = 0.8$ V; $V_R = 31$ V)	$C'_j = 32$

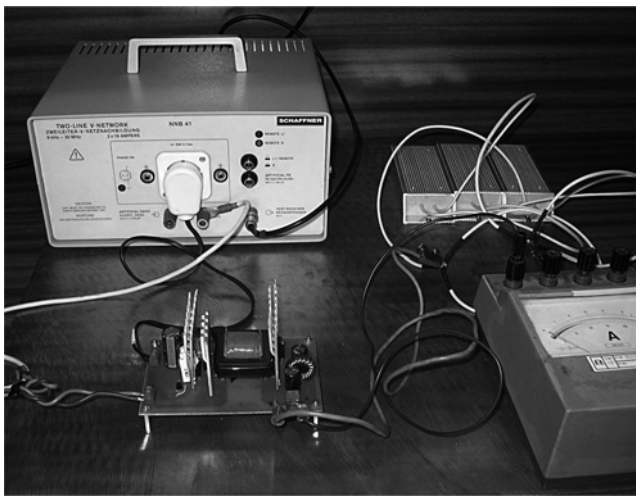

Fig. 4 *Flyback converter prototype, LISN and load*

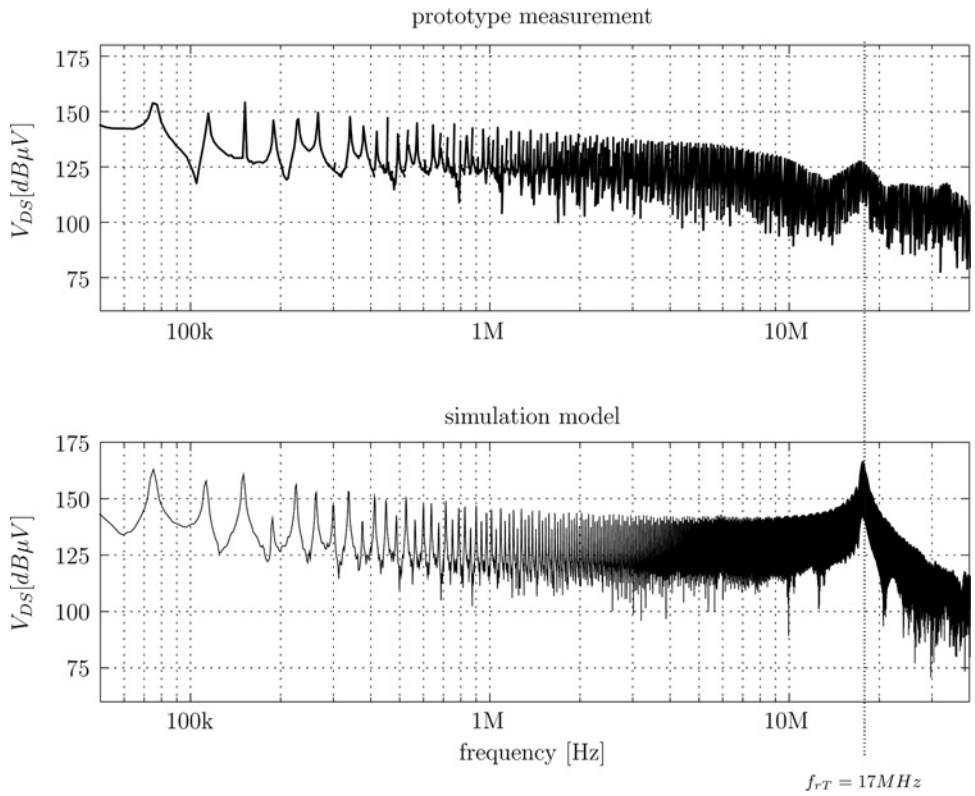

Fig. 5 *Simulated and measured transistor V_{ds} voltage FFT spectra (without snubber)*

coherence in the lower frequency range up to a few MHz where envelopes for both signals have similar shape, but for the higher frequencies, experimental spectra envelopes indicate less emission levels than simulated ones of about 20–30 dBμV. This can be caused by neglecting parasitic resistance of connections and components which increase for high frequencies because of skin effect. However, the main advantage of the simulation approach is a precise prediction of the EMI peak frequencies corresponding to turn-off of the MOSFET (17.4 MHz) and the diode (30.7 MHz) ringing frequencies.

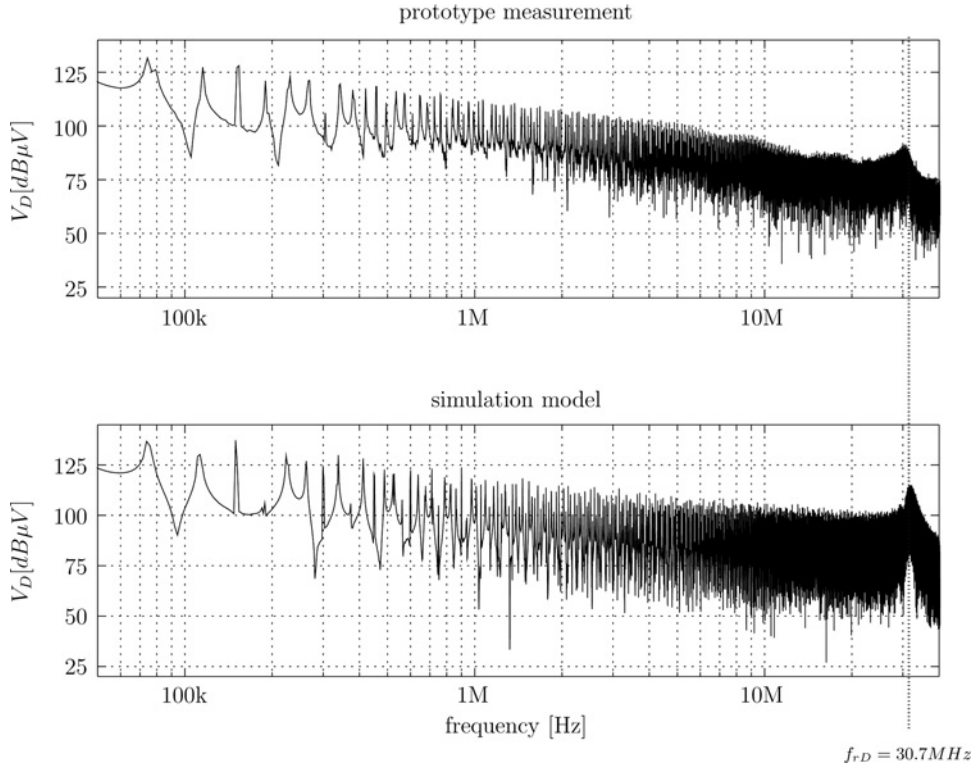

Fig. 6 *Simulated and measured diode V_d voltage FFT spectra (without snubber)*

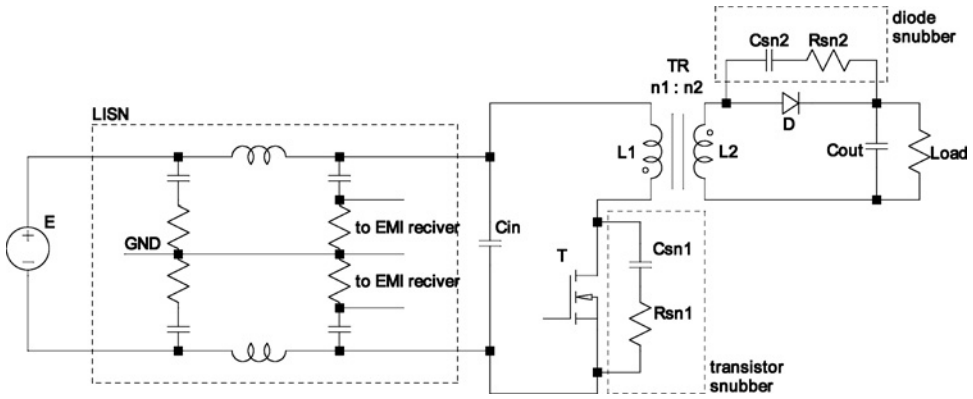

Fig. 7 *EMI noise measurement setup for a Flyback converter*

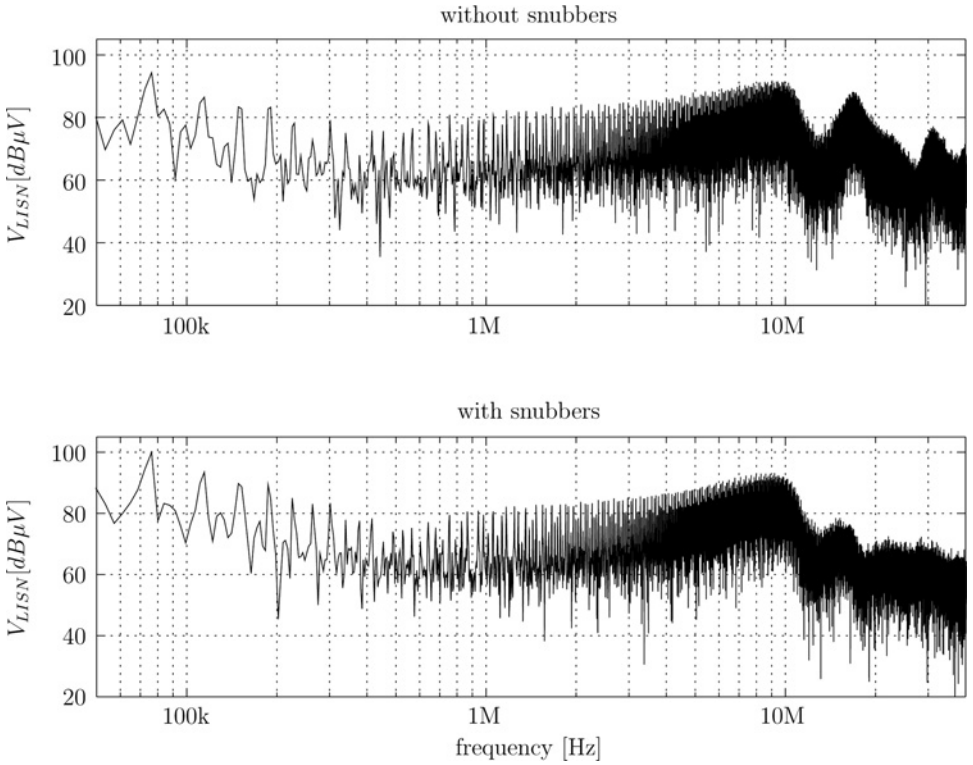

Fig. 8 *Conducted EMI spectra of a flyback converter without snubbers and after snubbers application*

4 Snubber design application

Following design recommendation [14, 22] two snubbers have been applied: transistor RC snubber damping $f_{rT} = 17.4$ MHz oscillations at the transistor turn off, and the diode RC snubber damping $f_{rD} = 30.7$ MHz oscillations at the diode turn off. For all calculation, transformer leakage inductances, measured at converter switching frequency (f_s), will be needed.

Parameters both for transistor and diode, snubber circuit (Fig. 7) [22] are given by

$$\mathrm{Rsn} = 2\pi f_r L_l \tag{4}$$

$$\mathrm{Csn} = \frac{1}{2\pi f_r \mathrm{Rsn}} \tag{5}$$

where, L_l is leakage inductance (primary for transistor snubber, secondary ($L1_l/n^2$) for diode snubber), f_r is transistor or diode ringing frequency.

In Fig. 8 the LISN spectra of the experimental flyback converter before and after snubber applied are compared. Top figure window depicting converter operation without snubbers, the characteristic transistor and diode turn–off EMI frequencies are transparent. In the bottom figure window, when the snubber have been applied on the transistor and diode terminals, the disturbances of the considered turn-off ringing frequencies of the MOSFET and the diode have been significantly cut off. Experimental comparison of the MOSFET V_{ds} voltage turn-off transients in Fig. 9 confirms effective damp down ringing frequency after snubber application. It is however evident the initial V_{ds} peak voltage resting unaltered. If it is necessary to limit this over voltage, the additional RCD clamp circuit should be applied [22–24].

5 Conclusion

Effective design of snubbers in a flyback converter is based on commutation EMI frequencies prediction obtained from circuit oriented simulation. For this purpose converter model reduction is

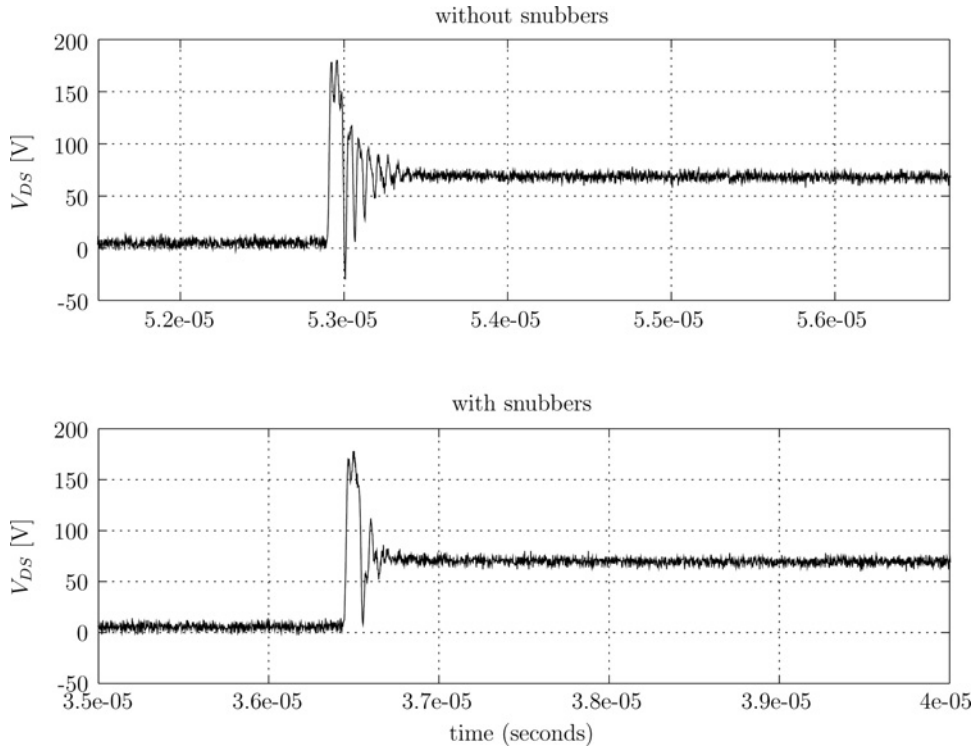

Fig. 9 *MOSFET turn-off voltage V_{ds} transients – before and after snubber application*

developed by using equivalent capacitive models of MOSFET and diode switches. Indeed, semiconductor capacitances and transformer leakage inductance have most significant impact on the turn off ringing frequencies. Moreover, these parameters can be directly derived from manufacturer datasheets. Wheras, parasitic transformer capacitances and the PCB parasitic inductances in properly designed converter layout are insignificant and can be neglected. Validation tests carried out in a laboratory setup have proved agreement of experimental MOSFET and diode switches spectra with those obtained from simulation tests. Comparative LISN spectra confirmed effective attenuation of the MOSFET and the diode turn-off ringing frequencies. Application of that way predicted EMI frequencies to snubbers sizing enabled less time consuming design of a presented flyback converter.

6 References

1 Emami, Z., Farzanefard, H., Motahari, S.: 'Precise prediction of conducted EMI in PWM flyback converters'. 18th Iranian Conf. on Electrical Engineering (ICEE), May 2010, pp. 765–771

2 Longtao, L., Lixin, W., Chao, L., Chao, S.: 'A simulation of conducted EMI in flyback converters'. Seventh Int. Power Electronics and Motion Control Conf. (IPEMC), June 2012, vol. 3, pp. 1794–1798

3 Yazdani, M., Farzanehfard, H., Faiz, J.: 'Conducted EMI modeling and reduction in a flyback switched mode power supply'. Second Power Electronics, Drive Systems and Technologies Conf. (PEDSTC), February 2011, pp. 620–624

4 Britto, K., Dhanasekaran, R., Vimala, R., Saranya, B.: 'EMI analysis and evaluation of an improved flyback converter'. Int. Conf. on Computer Communication and Informatics (ICCCI), January 2012, pp. 1–7

5 Karvonen, A., Thiringer, T.: 'Simulating the EMI characteristics of flyback DC/DC converters'. IEEE 33rd Int. Telecommunications Energy Conf. (INTELEC), October 2011, pp. 1–7

6 Yazdani, M., Farzanehfard, H.: 'Conducted electromagnetic interference analysis and mitigation using zero-current transition soft switching and spread spectrum techniques', *IET Power Electron.,* 2012, **5**, (7), pp. 1034–1041

7 Wang, Q., An, Z., Zheng, Y., Yang, Y.: 'Parameter extraction of conducted electromagnetic interference prediction model and optimisation design for a DC-DC converter system', *IET Power Electron.*, 2013, **6**, (7), pp. 1449–1461

8 Britto, K.R.A., Dhanasekaran, R., Vimala, R., Saranya, B.: 'Modeling of conducted EMI in flyback switching power converters'. Int. Conf. on Recent Advancements in Electrical, Electronics and Control Engineering (ICONRAEeCE), 2011, pp. 377–383

9 Mugur, P., Roudet, J., Crebier, J.-C.: 'Power electronic converter EMC analysis through state variable approach techniques', *IEEE Trans. Electromagn. Compat.*, 2001, **43**, (2), pp. 229–238

10 Yazdani, M., Filabadi, N., Faiz, J.: 'Conducted electromagnetic interference evaluation of forward converter with symmetric topology and passive filter', *IET Power Electron.* 2014, **7**, (5), pp. 1113–1120

11 Wooding, G.N., De Beer, A.: 'The effect of leakage inductance and snubbing on electromagnetic interference generated by a flyback converter'. AFRICON, September 2011, pp. 1–5

12 Popova, L., Juntunen, R., Musikka, T., *et al.*: 'Stray inductance estimation with detailed model of the IGBT module'. 15th European Conf. on Power Electronics and Applications (EPE), September 2013, pp. 1–8

13 Pong, M., Lee, C.M., Wu, X.: 'EMI due to electric field coupling on PCB'. 29th Annual IEEE Power Electronics Specialists Conf., PESC 98 Record, May 1998, vol. 2, pp. 1125–1130

14 Picard, J.: 'Under the hood of flyback SMPS designs'. Texas Instruments Power Supply Design Seminar, 2010

15 Mohammadi, M., Adib, E., Farzanehfard, H.: 'Lossless passive snubber for double ended flyback converter with passive clamp circuit', *IET Power Electron.* 2014, **7**, (2), pp. 245–250

16 Yang, Y., Wang, Z.-J., Cai, X., Wang, Z.: 'Improved lumped parameter model for transformer fast transient simulations', *IET Electr. Power Appl.,* 2011, **5**, (6), pp. 479–485

17 Meng, P., Zhang, J., Chen, H., Qian, Z., Shen, Y.: 'Characterizing noise source and coupling path in flyback converter for common-mode noise prediction'. 26th Annual IEEE Applied Power Electronics Conf. and Exposition (APEC), 2011, pp. 1704–1709

18 Maas, S.A.: 'Nonlinear microwave and RF circuits' (Artech House, 2003)

19 Musznicki, P., Schanen, J.-L., Granjon, P., Chrzan, P.: 'The Wiener filter applied to EMI decomposition', *IEEE Trans. Power Electron.*, 2008, **23**, (6), pp. 3088–3093

20 Kraft, C.: 'Conducted noise from 48 volt dc-dc converters used in telecommunications systems and its mitigation for emc'. Third Int. Telecommunications Energy Special Conf. TELESCON 2000, pp. 327–331

21 Tarateeraseth, V., Maneenopphon, T., Khan-ngern, W.: 'The comparison of EMI and electrical performances of high frequency transformer windings for SMPS applications'. Power Conversion Conf. – Nagoya, PCC'07, 2007, pp. 435–440

22 Ridley, R.: 'Flyback converter snubber design'. Switching Power Magazine, 2005, pp. 1–7

23 Jung, J.-H., Ahmed, S.: 'Flyback converter with novel active clamp control and secondary side post regulator for low standby power consumption under high-efficiency operation', *IET Power Electron.* 2011, **4**, (9), pp. 1058–1067

24 Hren, A., Korelic, J., Milanovic, M.: 'Rc-rcd clamp circuit for ringing losses reduction in a flyback converter', *IEEE Trans. Circuits Syst. II: Express Briefs,* 2006, **53**, (5), pp. 369–373